Eur Biophys J (2005) 34: 314–322
DOI 10.1007/s00249-004-0452-x

ARTICLE

Marcel Aguilella-Arzo · Vicente M. Aguilella
R. S. Eisenberg

Computing numerically the access resistance of a pore

Received: 9 September 2004 / Revised: 22 October 2004 / Accepted: 23 November 2004 / Published online: 9 March 2005

Abstract The access resistance (AR) of a channel is an important component of the conductance of ion channels, particularly in wide and short channels, where it accounts for a substantial fraction of the total resistance to the movement of ions. The AR is usually calculated by using a classical and simple expression derived by Hall from electrostatics (J.E. Hall 1975 *J. Gen. Phys.* 66:531–532), though other expressions, both analytical and numerical, have been proposed. Here we report some numerical results for the AR of a channel obtained by solving the Poisson–Nernst–Planck equations at the entrance of a circular pore. Agreement is found between numerical calculations and analytical results from Hall's equation for uncharged pores in neutral membranes. However, for channels embedded in charged membranes, Hall's expression overestimates the AR, which is much lower and can even be neglected in some cases. The weak dependence of AR on the pore radius for charged membranes at low salt concentration can be exploited to separate the channel and the access contributions to the measured conductance.

Keywords Access resistance · Channel conductance · Membrane pore · Poisson–Nernst–Planck equations

Introduction

Conductance measurements are routinely performed on ion channels to help characterize the translocation of charged solutes across biological membranes. Single-channel conductance has been used to explore the geometry of the pore lumen of a number of ion channels (Hille 2001), and inversely, their conductance properties have been predicted on the basis of channel structural data (Smart et al. 1998; Schirmer and Phale 1999; Im and Roux 2002; Chung and Kuyucak 2002), though both methodologies face several problems. Solute-exclusion experiments, using water-soluble polymers, are very often combined with measurements of ionic conductance to evaluate the size of the pores (Rostovtseva et al. 2002, and references therein), although it is well known that direct estimation of the pore geometry requires elaborate techniques (Merzlyak et al. 1999) and substantial problems arise because of the sensitivity of the predicted conductance to details of structure (Allen et al. 2003, 2004; Hollerbach and coworkers 1999, 2001; Mamonov et al. 2003; Eisenberg 1996). All these experiments require a correct interpretation of the factors contributing to the channel conductance. Besides, ion conduction from bulk solution to a confined geometry like an ion channel involves a convergence of the electric current flux lines and the idea of a pore entrance-related resistance.

The access resistance (AR) of a channel is defined as the electrical resistance along the convergent paths from the bulk medium to the end of a pore (Hille 2001) and can become a significant contribution in ion channels, which are both short and wide (Fig. 1). For example, at low-ion concentration or high-applied potential, electrodiffusion near the channel entrance can be the rate-controlling step for channel conductance rather than the intrinsic channel properties (Läuger 1976). There are channels for which AR is supposed to limit the flux of ions and consequently control the properties of the channel (Song et al. 1999). However, in most common cases, the AR of both channel apertures contributes between 10 and 30 % to the overall channel resistance (Bezrukov and Vodyanov 1993; Carneiro et al. 2003). AR is not easy to measure because of the intrinsic difficulty in separating it from the channel contribution. This impediment has been ingeniously circumvented by

M. Aguilella-Arzo · V. M. Aguilella (✉)
Biophysics Unit, Department of Experimental Science,
Universitat Jaume I, Castellón, 12080, Spain
E-mail: aguilell@exp.uji.es
Fax: +34-964-728066

R. S. Eisenberg
Department of Molecular Biophysics,
Rush University Medical Center, Chicago, IL, USA

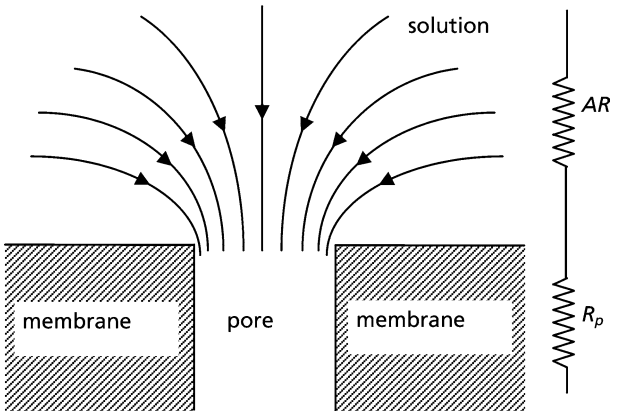

Fig. 1 Ion flux lines approach each other near the pore mouth. The contribution of the outer region is known as access resistance (AR) and can become of the same order of magnitude as the resistance of the channel proper

performing different conductance measurements with salt solutions containing water-soluble polymers (Vodyanov et al. 1992; Bezrukov and Vodyanov 1993). Furthermore, these authors estimated the size of ion channels by using a simple analytical expression for AR, proposed by Hall (1975).

Predicting theoretically the AR of an ion channel requires detailed knowledge of the structure of the end of the channel as well as solving the electrodiffusion equations at the channel–solution interface, by using suitable boundary conditions (size and shape of the openings, membrane fixed charges, channel charged residues, applied voltage, etc.). The structure of the channel-forming protein and the shape of its opening at the membrane–solution interface is not known at the microscopic level, except for a few proteins whose crystal structure has been resolved by X-ray diffraction. Hence, it is usual to consider a circular pore on the plane of the membrane surface.

In computing resistance, the simplest choice is using Ohm's law for a homogeneous conducting medium. Note that this implies assuming a noncharged membrane surface and also a neutral pore. This is basically the approach used by Hille (1967, 1968), who approximated the AR as the resistance of a region comprised between a spherical surface centered at the end of the pore with radius equal to that of the pore and a surface located at infinity. This result was later corrected by Hall (1975), who found that the resistance of the hemisphere close to the pore is of the same order as the remaining infinite sphere. With the assumption that the end of the circular pore is an equipotential surface, and using the theory of ohmic conductors, Hall gave a simple, analytical expression for the AR of a channel that has become a classic in channel conductance studies:

$$R_{\mathrm{Hall}} = \frac{1}{4a\kappa}, \tag{1}$$

where κ is the homogeneous conductivity of the solution near the pore and a is the radius of the end of the pore. Equation 1 is widely used in the literature, applied to different channels (Vodyanov et al. 1992; Bezrukov and Vodyanov 1993; Zambrowicz and Colombini 1993; Corry et al. 2000; Carneiro et al. 2003), either explicitly, in calculations of AR, or implicitly, when it is assumed that AR varies inversely with the pore radius while the resistance of the channel proper varies inversely with the radius squared. Equation 1 will be used as a reference throughout this work.

It is worth noting that Hall's expression, derived from electrostatics, is formally similar to the equation for convergence resistance to a conducting circular disk in an infinite conducting medium, and can be found in classical texts of electricity and magnetism (Jeans 1960) as well as in other monographs devoted to the solution of specific physical problems (Gray and Mathews 1922). Furthermore, as early as in the nineteenth century, Lord Rayleigh (1945) reported an expression similar to Eq. 1, within the context of sound propagation near the circular aperture of a cylindrical tube. More recently, Engel et al. (1972) analyzed the electrostatic potential created by a microelectrode (physically, a source of current) inside a spherical cell. In their work they discussed the concept of "convergence resistance" for current flowing spherically away from the electrode and were aware of Hall's formula (Eisenberg and Engel 1970) from the classical references previously cited.[1] Interestingly, they found the AR was related to two physically different effects: one coming from the nonuniformity of flux and the other from the potential drop across the cytoplasm.

Läuger (1976) extended Hall's treatment and analyzed the diffusion-limited ion flow in the vicinities of the pore entrance. His solution of Nernst–Planck flux equations was restricted to the case of no charges either within the pore or on the membrane surface. The spherical symmetry outside the pore and the assumption of electroneutrality of the solution near the pore entrance allowed him to find an analytical solution in a few simple and relevant cases.

A more elaborate procedure was reported by Peskoff and Bers (1988), who solved the Poisson and Nernst–Planck (PNP) equations simultaneously. Nevertheless, their treatment had two limitations: it considered an ideally selective channel and it did not include the hemisphere close to the end of the pore. Furthermore, they assumed spherical symmetry, which would be a good approximation far from the channel but is expected to fail near the pore or in case of a channel embedded in a charged membrane.

Levadny et al. (1998) introduced a model that takes into account the hemisphere near the pore, but assumed straight flux lines inside this region and spherical symmetry outside it. They solved 1D PNP equations to estimate the fluxes. As the authors note, their approach

[1] Historical note: it is not clear if Hall knew of the work of Eisenberg and Engel or of the classical work cited above. G. Szabo, a coworker of Hall and colleague of Eisenberg, was certainly aware of it.

is only valid for low ion fluxes and not very high channel ion selectivity.

Issues of AR and boundary conditions have also been considered by Nonner and Eisenberg (1998), Gillespie and Eisenberg (2001, 2002) and Romao and Price (1996).

It is noteworthy that all the approaches just described, which do not predict noticeable deviations from Hall's AR values, are only valid for noncharged channels embedded in neutral or weakly charged membranes. However, conductance measurements in charged channels as well as in neutral channels embedded in charged lipid membranes are very common. By using a continuum electrodiffusion model here, we numerically evaluate AR under several conditions of salt concentration, channel fixed charge density, membrane surface charge density and pore radius. The aim is computing the AR of a channel from a more general perspective and comparing the results with those obtained using Hall's expression. We solve the full set of PNP equations numerically at the entrance of a cylindrical channel and account for the convergence resistance arising from the gradients of ion concentration and electric potential.

There have been many notable attempts to solve the PNP equations. Kurnikova et al. (1999) solved the full 3D set of PNP equations for a gramicidin A channel, though they did not include the region immediately outside the channel. Hollerbach and coworkers(1999, 2001), working independently, included enough bathing solution to overcome the artificial boundary conditions used in the previous model. In this case the spectral element method was used, instead of a finite-difference method and issues of convergence were dealt with in some detail (Hollerbach et al. 2001) in the tradition of numerical analysis (Bank et al. 1990; Damocles 1999; Gummel 1964; Jerome 1995; Kerkhoven 1988; Kerkhoven and Saad 1992; Scharfetter and Gummel 1969; Selberherr 1984).

Im and Roux (2002) used Kurnikova's approach to compare results obtained by means of molecular dynamics and Brownian dynamics to those found with PNP equations in OmpF porin, and found good agreement between the three approaches.

It is still unclear how far continuum theories can be applied to systems with sizes comparable to that of atoms and these matters are under active investigation in many laboratories. Following the work of Kurnikova et al., Corry et al. (2000) tested Brownian dynamics against PNP and Poisson–Boltzmann theories and found the latter to overestimate shielding effects by counterions inside the pore. For recent work, see, for example, Cardenas et al. (2000), Graf et al. (2000), Kurnikova et al. (1999), Mamonov et al. (2003), Corry et al. (2003), Edwards et al. (2002) and Schuss et al. (2001). Other important effects have also been investigated and included in modified PNP versions. For example, PNP in its original formulation in biophysics (Barcilon 1992; Barcilon et al. 1992; Chen et al. 1992, 1993; Eisenberg 1996) did not take proper account of the dielectric boundary force (Nadler 2003) because of its physically naïve reduction in dimensionality, unknowingly following the history of computational electronics (Grasser et al. 2003; Jacoboni et al. 1989; Selberherr 1984), as was originally pointed out by Dieckman, Chung and Coalson's group at more or less the same time (Dieckmann et al. 1999; Corry et al. 1999; Kurnikova et al. 1999; Graf et al. 2000). The proper treatment of the dielectric boundary force is under active investigation in many groups because it captures many of the effects of the shape of the protein and its channel (Aboud et al. 2004; Boda et al. 2004; Cardenas et al. 2000; Chung et al. 1999; Corry et al. 1999, 2003; Dieckmann et al. 1999; Graf et al. 2000; Im et al. 2001; Kurnikova et al. 1999; Mamonov et al. 2003; Moy et al. 2000; Nadler and coworkers 2003, 2004a, 2004b). Since we perform PNP calculations in the region just outside the pore, away from a dielectric boundary, these limitations are not likely to influence the results presented here (Nadler et al. 2003, Fig. 1). In addition, the effect of the reaction field inside wide channels (radius close to 1 nm, when the contribution of AR becomes significant) is almost negligible (Corry et al. 2000).

Model

Let us assume a cylindrical channel of radius a embedded in a planar lipid membrane. There may be fixed-charge groups either on the pore wall or on the membrane–solution surface.

The equations that describe the flux of ions through the pore and solution are Poisson's equation from electrostatics and Nernst–Planck's equations giving the flux of ions in terms of the generalized forces acting on them. They read, respectively,

$$\nabla^2\phi = -\frac{\rho}{\varepsilon}, \tag{2}$$

$$\vec{J}_i = -D_i\left(\vec{\nabla}c_i + \frac{z_i e}{kT}c_i\vec{\nabla}\phi\right), \tag{3}$$

where ρ stands for the total volume density of electric charge, ε is the electric permittivity, ϕ is the electrostatic potential and c_i is the local concentration of ionic species i. Here ρ, ϕ and c_i are local functions of the position in the solution, but we will omit explicit reference to this dependence to simplify the notation. Subindex i spans up to N present ionic species. k is the Boltzmann constant, e is the positive elementary charge and z_i is the charge number. We use the symbol ∇^2 for the Laplacian operator and $\vec{\nabla}$ for the gradient operator. These equations are coupled, since charge density ρ can be written as:

$$\rho = eN_{\mathrm{A}}\sum z_i c_i, \tag{4}$$

where N_{A} is the Avogadro number. The sum is over the ionic species (i) present in solution. We cannot solve

these equations directly because the fluxes $\vec{J}_i$ depend on position and are unknown. Additional information is provided by the continuity equation under the assumption of steady state (also known as Smoluchowski's equation):

$$\vec{\nabla}\vec{J}_i = 0. \tag{5}$$

By substituting Eq. 4 into Eq. 2 and using Eq. 5 over Eq. 3 we obtain

$$\begin{aligned} &\nabla^2\phi = -\tfrac{F}{\varepsilon}\sum z_i c_i, \\ &\vec{\nabla}\left(\vec{\nabla}c_i + \tfrac{z_i F}{RT}\vec{\nabla}\phi\right) = 0. \end{aligned} \tag{6}$$

For the purpose of numerical computation, it is convenient to write these equations by using dimensionless variables defined as

$$\begin{aligned} &c_i = c_{\text{bulk}}\bar{c}_i; \quad \lambda^{-2} = \frac{e^2 N_{\text{A}} c_{\text{bulk}}}{kT\varepsilon}; \quad X = \frac{x}{\lambda}; \quad R = \frac{r}{\lambda}; \\ &\varphi = \frac{e\phi}{kT}. \end{aligned} \tag{7}$$

Note that distances are scaled to the Debye length λ. Substitution of these new variables into Eq. 6 gives

$$\begin{aligned} &\nabla^2\varphi = \sum z_i\bar{c}_i, \\ &\vec{\nabla}\left(\vec{\nabla}\bar{c}_i + z_i\bar{c}_i\vec{\nabla}\varphi\right) = 0. \end{aligned} \tag{8}$$

For convenience, we introduce the so-called *Slotboom* change of function (Selberherr 1984; Jerome 1996), so that a new variable γ_i is defined as

$$\bar{c}_i \equiv \gamma_i \mathrm{e}^{-z_i\varphi}, \tag{9}$$

which further simplifies our equations leading to

$$\begin{aligned} &\nabla^2\varphi = \sum z_i\gamma_i\mathrm{e}^{-z_i\varphi}, \\ &\vec{\nabla}\left(\mathrm{e}^{-z_i\varphi}\vec{\nabla}\gamma_i\right) = 0. \end{aligned} \tag{10}$$

The cylindrical symmetry demands the use of cylindrical coordinates. The channel axis is chosen as the x-axis with the origin located at the center of the circle representing the channel entrance. We get finally in cylindrical coordinates

$$\begin{aligned} &\tfrac{1}{R}\tfrac{\partial}{\partial R}\left(R\tfrac{\partial\varphi}{\partial R}\right) + \tfrac{\partial^2\varphi}{\partial X^2} = \sum z_i\gamma_i\mathrm{e}^{-z_i\varphi}, \\ &\vec{\nabla}\left[\left(\tfrac{\partial\gamma_i}{\partial R},\ 0,\ \tfrac{\partial\gamma_i}{\partial X}\right)\mathrm{e}^{-z_i\varphi}\right] = 0. \end{aligned} \tag{11}$$

In Eq. 11, we do not write explicitly the divergence operator, as we will need to use a special treatment for it when solving numerically this system of equations. Also, the assumed cylindrical symmetry makes the PNP equations independent of the angular coordinate, so we have $(N+1)$ 2D partial differential equations that should be solved simultaneously over the selected coordinate ranges. Hereafter, we will assume $N=2$ (e.g., a 1:1 electrolyte like NaCl).

For solving PNP Eq. 11, we select the finite-size box shown in Fig. 2 (see the domain for computation enlarged). It is large enough for the following boundary conditions to be approximately valid. First, from the cylindrical symmetry it follows

$$\frac{\partial\varphi}{\partial R} = 0; \quad \frac{\partial\gamma_i}{\partial R} = 0 \text{ at } R = 0. \tag{12}$$

Second, far from the pore, at a distance $L\lambda$ (much greater than the channel size) in the radial and axial directions, we can assume constant potential or their derivative and concentrations, that is,

$$\begin{aligned} &\gamma_i = 1; \quad \varphi = 0 \quad \text{for } X = L, \text{ any } R, \\ &\gamma_i = 1; \quad \tfrac{\partial\varphi}{\partial R} = 0 \quad \text{for } R = L, \text{ any } X. \end{aligned} \tag{13}$$

At $X=0$, we have two regions: the end of the pore and the membrane surface. At the pore entrance the electric potential and the concentrations are not known a priori, so we introduce new parameters γ_i^{mouth} and V, which will be estimated later.

$$\left.\begin{aligned} &\gamma_1 = \gamma_1^{\text{mouth}} \\ &\gamma_2 = \gamma_2^{\text{mouth}} \\ &\varphi = V \end{aligned}\right\} \quad \text{for } X = 0 \text{ and } R < a \tag{14}$$

At the membrane surface (assumed to be impermeable to ions) ion fluxes vanish. In addition, we use Gauss's theorem as a boundary condition for the electrostatic potential (the assumption of negligibly small potential and/or low dielectric inside the lipid membrane is implicit). Then, we have

$$\left.\begin{aligned} &\tfrac{\partial\varphi}{\partial X} = -\tfrac{e\sigma\lambda}{kT\varepsilon} \\ &\tfrac{\partial\gamma_i}{\partial X} = 0 \end{aligned}\right\} \quad \text{for } X = 0 \text{ and } R \geqslant a, \tag{15}$$

where σ is the surface charge density. The set of Eqs. 11 with boundary conditions Eqs. 12, 13, 14 and 15 cannot be solved analytically, so we use a numerical approach based on a finite-difference method, together with a Gummel iteration. That is, we solve the Poisson equation for a guessed γ_i and use this potential profile ϕ in

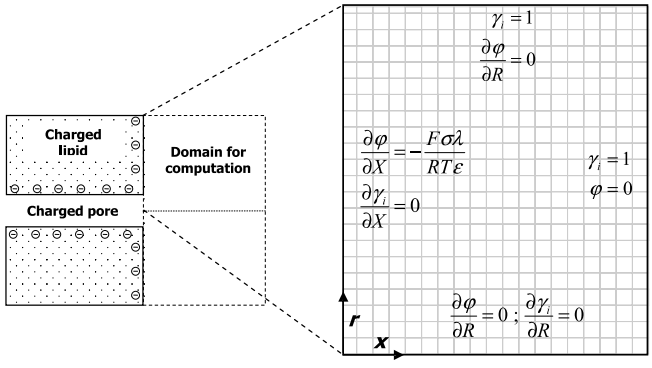

Fig. 2 Simplified view of the model used to compute AR. A charged pore of radius a immersed in a charged membrane and bathed by an ionic solution. The computational domain shown includes a portion of the solution located near the mouth of the channel. Boundary conditions are included

the Nernst–Planck equations to get improved values for γ_i. This procedure is then repeated several times until convergence is reached. This convergence can be checked computing the residues of the difference equations.

One important point that we need to take into account when discretizing the set of Eqs. 11 is the use of a conservative approach, which preserves the physical meaning of divergence. To this end, we build a rectangular mesh over our numerical box. We consider a basic cell around a point of our mesh (Figs. 3), and apply Gauss's theorem to it. The continuity Eq. 5 for ionic species i, in the basic cell (m, n), can be written as

$$\begin{aligned}\left(\vec{\nabla}\cdot\vec{J}_i\right)_{m,n} &= J_{ri}^{m+\frac{1}{2},n}2\pi R_{m+\frac{1}{2}}\left(X_{n+\frac{1}{2}}-X_{n-\frac{1}{2}}\right)\\ &- J_{ri}^{m-\frac{1}{2},n}2\pi R_{m-\frac{1}{2}}\left(X_{n+\frac{1}{2}}-X_{n-\frac{1}{2}}\right)\\ &+ J_{zi}^{m,n+\frac{1}{2}}2\pi R_m\left(R_{m+\frac{1}{2}}-R_{m-\frac{1}{2}}\right)\\ &- J_{zi}^{m,n-\frac{1}{2}}2\pi R_m\left(R_{m+\frac{1}{2}}-R_{m-\frac{1}{2}}\right)=0\end{aligned} \tag{16}$$

where we have defined discretized radial and axial coordinates at each grid point as R_m and X_n. We should take into account that each grid cell is a "ring" in real space because of the axial symmetry (this is the origin of the term $2\pi R$ in Eq. 16). We substitute in this expression the difference approximation of

$$\begin{aligned}J_{ri} &= \frac{\partial\gamma_i}{\partial R}\mathrm{e}^{-z_i\varphi},\\ J_{xi} &= \frac{\partial\gamma_i}{\partial X}\mathrm{e}^{-z_i\varphi}\end{aligned} \tag{17}$$

to obtain the difference equivalent to the second equation in Eqs. 11 (Gummel 1964; Jerome 1995; Selberherr 1984).

In our case, we use a third-order upwind expression for Eq. 17 and for the first equation in Eqs. 11. We also check higher- and lower-order expressions, but our choice is the one that gives optimal results. Following this method, we obtain a potential and concentration profile near the end of the pore. These profiles are read with Mathematica and later used for calculating the electric flux crossing a surface that completely encloses the end of the pore, by using the simple relationship

$$I = \sum_i z_i F\int \vec{J}_i \mathrm{d}\vec{S}. \tag{18}$$

The AR is then simply $\mathrm{AR} = U/I$. In this equation, U is the difference between the potential naturally arising under equilibrium conditions at the end of the pore (in the absence of flux) and the boundary condition used to solve numerically the equations (V), as pointed out previously by Peskoff and Bers (1988). $\vec{J}_i$ is calculated from Eq. 3 using the calculated potential and concentration values and the bulk aqueous diffusion coefficients of the appropriate ions. Computations have been made under several conditions to check the range of validity of the widely used Hall expression. All calculations were performed with a Pentium 4, 2.4-GHz computer, with 512-MB memory. A grid of 128×128 points was enough for most of the computations, though in some cases it was necessary to increase it to 256×256 in order to get convergence. Before computing these cases, we tried to reproduce Hall's results by simulating the conditions for which it is valid, that is, a homogeneous solution around the pore in a neutral membrane and small fluxes. In all cases the accuracy was within 0.5%. NaCl electrolyte was used in all calculations, though our code can be easily modified to account for other binary or ternary electrolytes.

At this point, we still have to clarify what the selected values for $\gamma_i^{\mathrm{mouth}}$ and V in Eq. 14 are, in order to complete our set of boundary conditions. Correct values for these quantities can only be obtained by solving the full set of PNP equations in the whole system, and generally they would depend not only on the pore and membrane charge, concentrations, and radius of the pore but also on the fluxes crossing the entire system. Our simple approach, however, will use the classic Donnan expression for concentrations and potential near the end of the pore, provided we have the pore charge, radius and remaining parameters. When we have a charged membrane, Donnan magnitudes are not well defined and we use previous results for the potential profile near the pore by Aguilella and Bezrukov (2001). From this potential profile, concentrations are obtained by assuming equilibrium and using the classical Boltzmann equation. This procedure assumes equilibrium for the solution near the pore. It is clear that this would imply no fluxes and, therefore, the PNP equations would be nonsense. However, previous results from Gillespie and Eisenberg (2001) suggest that, at least at low fluxes, this approach leads to correct results and also that it is not necessary to use a more accurate expression for the potential at the end of the pore, in the cases that they studied. Additionally, the Donnan approach is often used to obtain boundary conditions for channel models, and it would be interesting to quantify the correction in this framework.

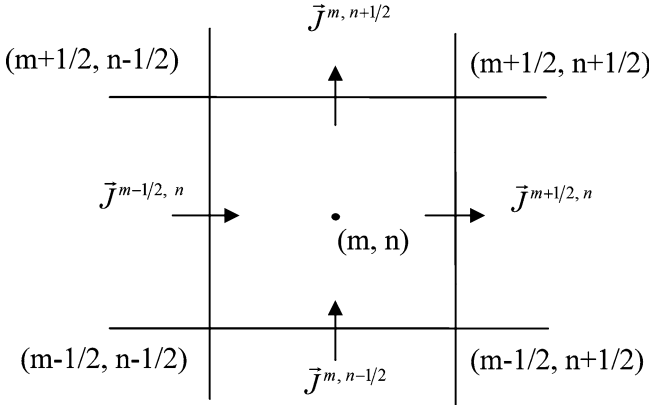

Fig. 3 A basic cell of the mesh used to solve the Poisson and Nernst–Planck equations. Gauss's theorem is applied to this cell to obtain a conservative form of the divergence operator

Results and discussion

In what follows, we use values of AR calculated according to Hall's equation, R_{Hall}, as a reference, and compare them with the numerical results of AR obtained with our model. $R_{\mathrm{Hall}} = 1/(4a\kappa)$ is the exact solution to the AR in the case of a homogeneous solution near a circular pore entrance on a neutral membrane, i.e., in the case of no charged membrane, neutral pore and very small fluxes.

Figure 4 shows the computed AR for a channel with radius 1 nm inserted in a charged membrane bathed by 0.1 M NaCl. The membrane charge density takes realistic values commonly found in charged lipid bilayers. For a neutral membrane, the numerically computed AR agrees with R_{Hall}. However, the AR is considerably reduced when the membrane is charged, either positively or negatively. The theoretical prediction for a strongly charged lipid bilayer (approximately 50 $\mathrm{Å}^2/e$) is a reduction of an order of magnitude with respect to AR in a neutral membrane. Also this decrease is almost independent of the sign of the membrane charge density.

The decrease of the AR as the membrane is more charged can be understood as a consequence of the counterion accumulation near the pore entrance because of the membrane surface charge. As a first approximation, the conductivity of the solution scales with the ionic concentration, i.e., with the number of available charge carriers, the salt ions: whatever changes this concentration should change the solution conductivity. The electric double layer near the membrane surface increases the conductivity of the solution, and hence the AR is decreased, as shown in Fig. 4.

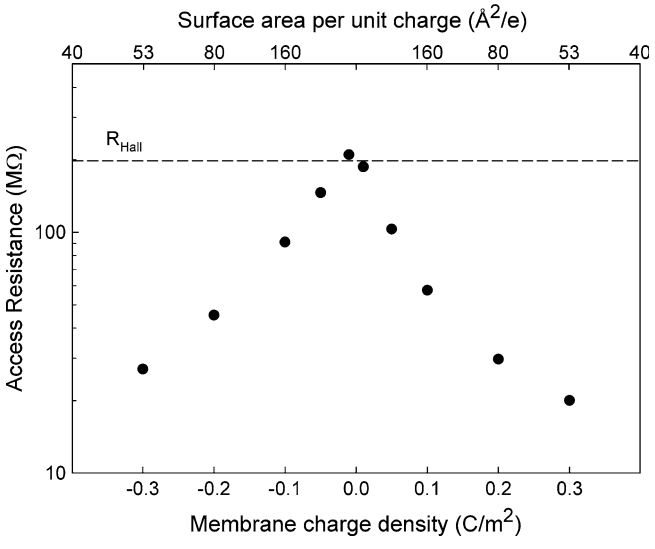

Fig. 4 AR for a channel with radius 1 nm inserted in a charged membrane bathed by 0.1 M NaCl. Both membrane charge density and its equivalent average surface area per elementary charge are shown. AR calculated using Hall's expression is shown as a *dashed line*. Values correspond to one pore entrance

There is nevertheless a small difference between the AR for pores embedded in a membrane with equal positive or negative surface charge density. It can be ascribed to the different diffusion coefficients of Cl^- and Na^+ ions: the diffusion coefficient of Na^+ is lower than that of Cl^-. Positively charged membranes will accumulate Cl^- ions near the pore entrance, and negatively charged membranes will do the same with Na^+ ions. However, the smaller mobility of cations compared with that of anions will be reflected in a greater AR in the latter case. As Fig. 4 shows, AR values corresponding to positive membrane charge densities are always below those corresponding to oppositely charged membranes.

The combination of both trends, that is, the effect of the different cation and anion diffusivities and that of the increase in the local concentration of counterions, has a different effect depending upon the sign of the fixed charge. In the case of a positively charged membrane, both effects produce a decrease of the AR with respect to the neutral case (R_{Hall}). In the case of negatively charged membranes, each effect goes in a different direction and it occurs that for slightly negative charge densities the diffusion coefficient effect dominates, giving an AR higher than that predicted by Hall (see in Fig. 4 that AR is slightly greater than R_{Hall} for a membrane charge density of 1 $\mathrm{mC/m^2}$). Higher charges in absolute value result in a overall reduction of the AR owing to the counterion accumulation.

Figure 5 shows the effect of the radius of aperture on the AR for a channel in a strongly charged membrane (-0.3 $\mathrm{C/m^2}$). Numerical results follow the same trend as R_{Hall}, i.e., a decrease in AR for increasing pore radius. However the dependence of AR with pore radius is weaker in our model. For 0.1 M NaCl, AR is almost insensitive to changes in the radius, while for 1 M NaCl the dependence is similar to that of $R_{\mathrm{Hall}} \propto 1/a$. This result is relevant to channel studies, which take advantage of the fact that the resistance of the channel proper roughly scales with $1/a^2$, while AR has a less steep dependence on the radius. The weaker the AR dependence on a, the easier it should be to separate the channel and access contributions (Bezrukov and Vodyanov 1993). Our model predictions show that this condition is best realized for channels inserted in charged membranes at low salt concentrations.

To understand this behavior, we must differentiate several solution regions in which the ion conduction takes place in the case of a charged membrane at high and low concentrations. At high salt concentration, the influence of the membrane spreads over very short distances from the wall, because of the ion screening. In this case, the ionic solution will hardly be influenced by the charges on the membrane and the situation will resemble that of a neutral unperturbed solution. Accordingly, $\mathrm{AR} \approx R_{\mathrm{Hall}}$. In contrast, at low concentration, screening will be weaker. Consequently, counterions will accumulate near the pore entrance and their concentration will be determined by the membrane charge, and will be largely independent of the bulk ion concentration. As

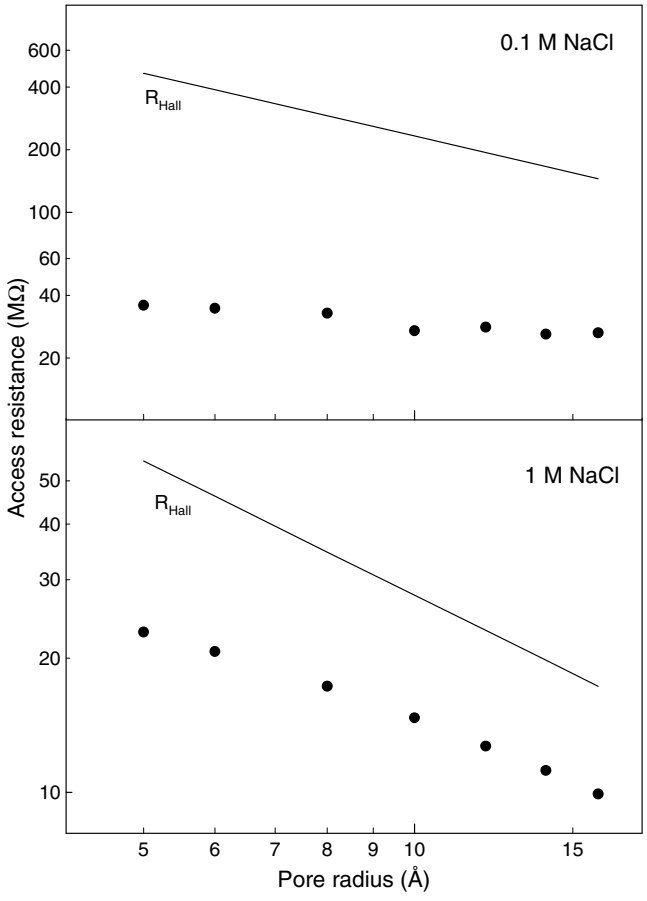

Fig. 5 AR as a function of the pore radius for a channel embedded on a charged membrane (-0.3 C/m^2) in NaCl solution. *Dots* are numerically computed values. *Solid lines* represent Hall's value (corrected for activities). Values correspond to one pore entrance

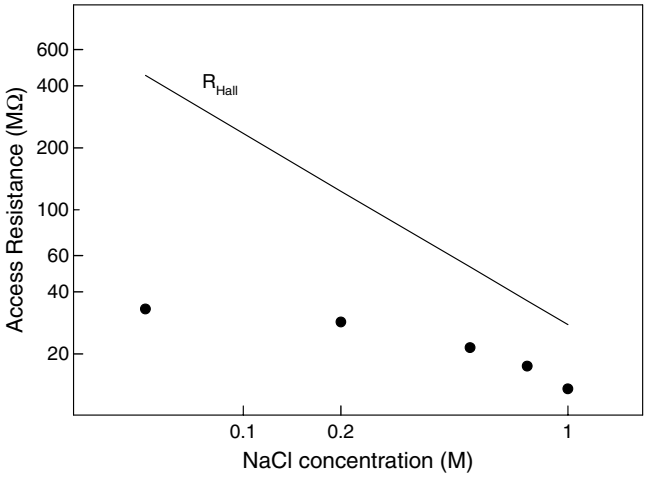

Fig. 6 AR versus solution concentration for a 10-Å-radius channel embedded on a negatively charged membrane (-0.3 C/m^2). The *solid line* represents Hall's prediction and *dots* correspond to our model calculations. Values correspond to one pore entrance

long as the Debye length of solution is similar to the pore radius, AR will be insensitive to the pore radius (Fig. 5, top panel).

Figure 6 shows the change of AR with salt concentration for a neutral pore in a strongly charged membrane (-0.3 C/m^2 or equivalently one elementary charge per average surface area of 50 Å^2, which is roughly the area per lipid molecule on a phospholipid bilayer). The difference between R_{Hall}, shown as a solid line, and numerical calculations of AR is bigger at low concentrations. The reason for this lies in the influence of the membrane charge density over a wider region as the concentration is lowered, since the Debye length of the solution increases at lower concentrations: the same effect discussed before for Fig. 4. At very low concentrations (approximately 0.05 M), the numerically computed AR is an order of magnitude below the reference value R_{Hall}. Given that R_{Hall} is at most 30% of the channel measured conductance, this result shown in Fig. 6 gives an indication that when conductance is measured in a channel inserted on a charged membrane, AR can be neglected.

In the results shown until now, we have assumed that the membrane in which the channel is inserted has a number of ionizable groups which polarize the solution near the channel entrance. It is this charge separation in the solution, what gives rise to the inhomogeneity that invalidates Hall's assumptions; therefore, AR deviates from R_{Hall}. However, it is also common to find channels with ionizable residues facing the pore lumen, which are partly responsible for their selectivity as well as for other electrokinetic phenomena. This charge inside the channel, like that on the membrane surface, can cause some inhomogeneity in the vicinity of the channel. This may happen if the fixed charges are located near the channel entrances. In Fig. 7 we show the numerical results for the AR of a charged channel with 10-Å radius as a function of the number of charges facing the pore lumen. In the calculations it is supposed that the channel has a length of 50 Å, which is the typical width of a lipid bilayer like that in cell membranes.

Figure 7 shows slightly different AR values for positive and negative pore charge for NaCl solution (circles). Positively charged pores tend to show smaller ARs than the value predicted from the Hall equation, while the negatively charged ones show a higher resistance. In fact, this behavior compares nicely to that found in the case of a charged membrane (Fig. 5) for small values of the charge density. What we see in Fig. 7 results from the different diffusion coefficients of positive (Na^+) and negative (Cl^-) ions. For positively charged pores, Cl^--mediated conduction dominates. As chloride has a higher diffusion coefficient, this gives a lower AR. For negatively charged pores the behavior is the opposite. The effects on the AR are much more modest since the typical charges of the pores are usually much smaller than those in membranes. The effect is not more than 15% of the value obtained with Hall's equation.

In order to make the effect of the diffusion coefficient more apparent, we also include in Fig. 7 values computed for KCl (triangles) together with the predicted Hall value (dotted horizontal line). K^+ and Cl^- have very similar diffusion coefficients, and then we should

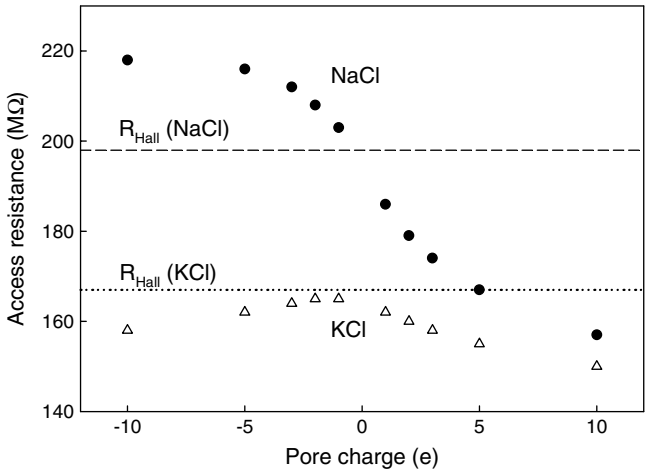

Fig. 7 AR (one pore entrance) for a charged channel inserted in a neutral membrane in 0.1 M NaCl (*circles*) and 0.1 M KCl (*triangles*) as a function of pore charge. The pore radius is 10 Å and the membrane thickness is assumed to be 50 Å. Hall's values are shown as a *dashed line* for NaCl and a *dotted line* for KCl

expect very similar conductivities no matter whether the cations or the anions are favored inside the channel. In this case, we recover the lowering of the AR already seen in Fig. 4 owing to the same effect: the increase in counterions produced by the pore charge in the vicinity of the pore, and consequently the increase in the number of carriers, decreases the AR.

We can conclude from these data that two opposite effects influence the AR in the general case: one coming from the pore charge, irrespective of its sign, which invariably reduces the value of the AR, and the other coming from the different diffusivities and the coion exclusion near the pore, which would increase or decrease the AR depending on the charge sign.

The model calculations presented here assume a circular aperture on the membrane surface. This is a rough but useful approximation that has been used in other studies of the influence of membrane charge on channel conductance (Rostovtseva et al. 1998; Aguilella and Bezrukov 2001). It is expected that channels with bulky entrances—e.g., the *Staphylococcus Aureus* α-hemolysin channel—would behave in a different way. The agreement between our model calculations and the AR predicted by Hall's expression is remarkable for uncharged pores in neutral membranes. Leaving apart this particular case, as a general trend, the computed values for AR are always lower than R_{Hall}, with the only exception being the case of a negatively charged pore inserted on a neutral membrane with NaCl electrolyte. However, the difference between the numerical and the analytical values is small (approximately 10%); therefore, the value for AR given by Hall's expression can be regarded as an upper limit in most cases of interest. Finally, it is interesting to note that the weak dependence of AR with the pore radius in charged membranes and low concentrations may be useful in experiments aimed at separating the channel and access contributions to the measured conductance.

Acknowledgements V.M.A. thanks the Fundació Caixa-Castelló (project P1-1B2001-20) and the MCYT (project BFM2001-3293) for their financial support. R.S.E. is grateful for support from the NIH, GM 067241. We thank A. Alcaraz for critically reading the manuscript and for his stimulating discussions, and Amit Singer for his useful comments and references.

References

Aboud S, Marreiro D, Saraniti M, Eisenberg R (2004) A Poisson P3M force field scheme for particle-based simulations of ionic liquids. J Comput Electron (in press)

Aguilella VM, Bezrukov SM (2001) Alamethicin channel conductance modified by lipid charge. Eur Biophys J 30:233–241

Allen TW, Andersen OS, Roux B (2003) Structure of gramicidin a in a lipid bilayer environment determined using molecular dynamics simulations and solid-state NMR data. J Am Chem Soc 125:9868–9877

Allen TW, Andersen OS, Roux B (2004) Energetics of ion conduction through the gramicidin channel. Proc Natl Acad Sci USA 101:117–122

Bank RE, Burgler J, Coughran WM Jr, Fichtner W, Smith RK (1990) Recent progress in algorithms for semiconductor device simulation. Int Ser Num Math 93:125–140

Barcilon V (1992) Ion flow through narrow membrane channels: part I. SIAM J Appl Math 52:1391–1404

Barcilon V, Chen DP, Eisenberg RS (1992) Ion flow through narrow membrane channels: part II. SIAM J Appl Math 52:1405–1425

Bezrukov SM, Vodyanoy I (1993) Probing alamethicin channels with water-soluble polymers. Effect on conductance of channel states. Biophys J 64:16–25

Boda D, Gillespie D, Nonner W, Henderson D, Eisenberg B (2004) Computing induced charges in inhomogeneous dielectric media: application in a Monte Carlo simulation of complex ionic systems. Phys Rev E Stat Nonlin Soft Matter Phys 69:046702

Cardenas AE, Coalson RD, Kurnikova MG (2000) Three-dimensional Poisson–Nernst–Planck studies. Influence of membrane electrostatics on gramicidin A channel conductance. Biophys J 79:80–93

Carneiro CMM, Merzlyak PG, Yuldasheva LN, Silva LG, Thinnes FP, Krasilnikov OV (2003) Probing the volume changes during voltage gating of Porin 31BM channel with nonelectrolyte polymers. Biochim Biophys Acta 1612:144–153

Chen DP, Eisenberg RS (1993) Charges, currents and potentials in ionic channels of one conformation. Biophys J 64:1405–1421

Chen DP, Barcilon V, Eisenberg RS (1992) Constant field and constant gradients in open ionic channels. Biophys J 61:1372–1393

Chung S-H, Kuyucak S (2002) Recent advances in ion channel research. Biochim Biophys Acta 1565:267–286

Chung S-H, Allen T, Hoyles M, Kuyucak S (1999) Permeation of ions across the potassium channel: Brownian dynamics studies. Biophys J 77:2517–2533

Corry B, Kuyucak S, Chung SH (1999) Test of Poisson–Nernst–Planck theory in ion channels. J Gen Physiol 114(4):597–599

Corry B, Kuyucak S, Chung S-H (2000) Tests of continuum theories as models of ion channels. II. Poisson–Nernst–Planck theory versus Brownian dynamics. Biophys J 78:2364–2381

Corry B, Kuyucak S, Chung SH (2003) Dielectric self-energy in Poisson–Boltzmann and Poisson–Nernst–Planck models of ion channels. Biophys J 84:3594–3606

Damocles (1999) Web address: http://www.research.ibm.com/DAMOCLES/html_files/sites.html

Dieckmann GR, Lear JD, Zhong Q, Klein ML, DeGrado WF, Sharp KA (1999) Exploration of the structural features defining the conduction properties of a synthetic ion channel. Biophys J 76:618–630

Edwards S, Corry B, Kuyucak S, Chung SH (2002) Continuum electrostatics fails to describe ion permeation in the gramicidin channel. Biophys J 83:1348–1360

Eisenberg RS (1996) Computing the field in proteins and channels. J Membr Biol 150:1–25
Eisenberg RS, Engel E (1970) The spatial variation of membrane potential near a small source of current in a spherical cell. J Gen Physiol 55:736–757
Engel E, Barcilon V, Eisenberg RS (1972) The interpretation of current-voltage relations recorded from a spherical cell with a single microelectrode. Biophys J 12:384–403
Gillespie D, Eisenberg RS (2001) Modified Donnan potentials for ion transport through biological ion channels. Phys Rev E 63:061902-1
Gillespie D, Eisenberg RS (2002) Physical descriptions of experimental selectivity measurements in ion channels. Eur Biophys J 31:454–466
Graf P, Nitzan A, Kurnikova MG, Coalson RD (2000) A dynamic lattice Monte Carlo model of ion transport in inhomogeneous dielectric environments: method and implementation. J Phys Chem B 104:12324–12338
Grasser T, Tang T-W, Kosina H, Selberherr S (2003) A review of hydrodynamic and energy-transport models for semiconductor device simulation. Proc IEEE 91(2):251–274
Gray A, Mathews GB (1922) A treatise on Bessel functions and their applications to physics. Dover Publications Inc., New York, p 143 (First published by McMillan and Co., London, 1922)
Gummel HK (1964) A self-consistent iterative scheme for one-dimensional steady-state transistor calculations. IEEE Trans Electron Devices 11:445–465
Hall JE (1975) Access resistance of a small circular pore. J Gen Phys 66:531–532
Hille B (1967) A pharmacological analysis of the ionic channels of nerve. PhD Thesis. The Rockefeller University; University Microfilms, Ann Arbor (Microfilm 68–9584)
Hille B (1968) Pharmacological modifications of the sodium channels of frog nerve. J Gen Physiol 51:199–219
Hille B (2001) Ionic channels of excitable membranes, 3rd edn. Sinauer Associates Inc., Sunderland
Hollerbach U, Chen D, Nonner W, Eisenberg B (1999) Three-dimensional Poisson–Nernst–Planck theory of open channels. Biophys J 76:A205
Hollerbach U, Chen D-P, Eisenberg RS (2001) Two- and three-dimensional Poisson–Nernst–Planck simulations of current flow through gramicidin-A. J Comp Sci 16:373–409
Im W, Roux B (2001) Brownian dynamics simulations of ions channels: a general treatment of electrostatic reaction fields for molecular pores of arbitrary geometry. Biophys J 115:4850–4861
Im W, Roux B (2002) Ion permeation and selectivity of OmpF porin: a theoretical study based on molecular dynamics, Brownian dynamics, and continuum electrodiffusion theory. J Mol Biol 322:851–869
Jacoboni C, Lugli P (1989) The Monte Carlo method for semiconductor device simulation. Springer, Berlin Heidelberg New York, pp 1–356
Jeans J (1960) The mathematical theory of electricity and magnetism. Cambridge University Press, London, p 195
Jerome JW (1995) Mathematical theory and approximation of semiconductor models. Springer, Berlin Heidelberg New York
Jerome JW (1996) Analysis of charge transport: a mathematical study of semiconductors. Springer, Berlin Heidelberg New York
Kerkhoven T (1998) On the effectiveness of Gummel's method. SIAM J Sci Stat Comp 9:48–60
Kerkhoven T, Saad Y (1992) On acceleration methods for coupled nonlinear elliptic systems. Numer Math 57:525–548
Kurnikova MG, Coalson RD, Graf P, Nitzan A (1999) A lattice relaxation algorithm for 3D Poisson–Nernst–Planck theory with application to ion transport through the gramicidin A channel. Biophys J 76:642–656
Läuger P (1976) Diffusion-limited ion flow through pores. Biochim Biophys Acta 455:493–509
Levadny V, Aguilella VM, Belaya M (1998) Access resistance of a single conducting membrane channel. Biochim Biophys Acta 1368:338–342
Mamonov AB, Coalson RD, Nitzan A, Kurnikova MG (2003) The role of the dielectric barrier in narrow biological channels: a novel composite approach to modeling single-channel currents. Biophys J 84:3646–3661
Merzlyak PG, Yuldasheva LN, Rodrigues CG, Carneiro CMM, Krasilnikov OV, Bezrukov SM (1999) Polymeric nonelectrolytes to probe pore geometry: application to the α-toxin transmembrane channel. Biophys J 77:3023–3033
Moy G, Corry B, Kuyucak S, Chung S (2000) Tests of continuum theories as models of ion channels. I. Poisson–Boltzmann theory versus Brownian dynamics. Biophys J 78:2349–2363
Nadler B, Hollerbach U, Eisenberg RS (2003) Dielectric boundary force and its crucial role in gramicidin. Phys Rev E Stat Nonlin Soft Matter Phys 68:021905
Nadler B, Schuss Z, Hollerbach U, Eisenberg RS (2004) Saturation of conductance in single ion channels: the blocking effect of the near reaction field. Phys Rev 70:051912
Nadler B, Schuss Z, Singer A, Eisenberg R (2004) Ionic diffusion through confined geometries: from Langevin equations to partial differential equations. J Phys Condens Matter 16:S2153-S2165
Nonner W, Eisenberg B (1998) Ion permeation and glutamate residues linked by Poisson–Nernst–Planck theory in L-type calcium channels. Biophys J 75:1287–1305
Peskoff A, Bers DM (1988) Electrodiffusion of ions approaching the mouth of a conducting membrane channel. Biophys J 53:863–875
Rayleigh JWS (1945) The theory of sound, vol 2, chap XVI. Dover, New York, pp170–183 (first edition 1878)
Romao JD, Price RH (1996) The conical resistor conundrum: a potential solution. Am J Phys 64:1150–1153
Rostovtseva TK, Aguilella VM, Vodyanoy I, Bezrukov SM, Parsegian VA (1998) Membrane surface-charge titration probed by gramicidin A channel conductance. Biophys J 75:1783–1792
Rostovtseva TK, Nestorovich EM, Bezrukov SM (2002) Partitioning of differently sized poly(ethylene glycol)s into OmpF porin. Biophys J 82:160–169
Scharfetter DL, Gummel HK (1969) Large signal analysis of a silicon read diode oscillator. IEEE Trans Electron Devices 16:64–77
Schirmer T, Phale PS (1999) Brownian dynamics simulation of ion flow through porin channels. J Mol Biol 294:1159–1167
Schuss Z, Nadler B, Eisenberg RS (2001) Derivation of PNP equations in bath and channel from a molecular model. Phys Rev E 64:036116-1
Selberherr S (1984) Analysis and simulation of semiconductor devices. Springer, Berlin Heidelberg New York
Smart OS, Coates GMP, Sansom MSP, Alder GM, Bashford CL (1998) Structure-based prediction of the conductance properties of ion channels. Faraday Discuss 111:185–189
Song J, Minetti CASA, Blake MS, Colombini M (1999) Meningococcal PorA/C1, a channel that combines high conductance and high selectivity. Biophys J 76:804–813
Vodyanoy I, Bezrukov SM, Colombini M (1992) Measurement of ion channel access resistance. Biophys J 61:A114
Zambrowicz EB, Colombini M (1993) Zero-current potentials in a large membrane channel—a simple theory accounts for complex behavior. Biophys J 65:1093–1100